Journal of Systemics, Cybernetics and Informatics (2023) 21(1), 73-79
https://doi.org/10.54808/JSCI.21.01.73

Movement of Cell Flowing over Oblique Microgroove

Shigehiro HASHIMOTO
Biomedical Engineering, Department of Mechanical Engineering, Kogakuin University
at13351@g.kogakuin.jp Tokyo, 163-8677, Japan

Shogo UEHARA
Biomedical Engineering, Systems Design, Kogakuin University
Tokyo, 163-8677, Japan

Natsuki MORIIZUMI
Biomedical Engineering, Department of Mechanical Engineering, Kogakuin University
Tokyo, 163-8677, Japan

ABSTRACT[1]

The bumping movement of the cell flowing over an oblique microgroove was analyzed *in vitro*. The micro flow-channel (0.05 mm high, 1 mm wide, 25 mm long) with rectangular grooves (4.5 μm deep, 0.2 mm long) was manufactured of polydimethylsiloxane (PDMS) by micromachining technique. The angle between the main flow direction and the longitudinal axis of the groove was 45 degrees. Three groove widths (0.03 mm, 0.04 mm, and 0.05 mm) were studied. Mouse myoblasts (C2C12 cell line) were used in the test. The bulk flow velocity (0.5 mm/s < v_c < 3 mm/s) of the medium was controlled by the pressure difference between the inlet and outlet. The centroid of each cell was tracked in a movie recorded by the camera attached on the eyepiece of the microscope. The experimental results show that the cell changes direction when passing over the oblique groove. The magnitude of the change depends on the flow velocity of the cell and on the width of the groove. The micro flow-channel with microgrooves has potential to be applied to sorting cells.

Keywords: Biomedical Engineering, C2C12, Micro Groove, Micro Flow Channel and Cell Movement.

1. INTRODUCTION

The technology of cell sorting is applied in diagnostic, therapeutic, and regenerative medicine; the key problem is to select the target cells [1, 2]. Several different methods have been proposed for sorting biological cells *in vitro*. Of course, a minimally invasive method is preferable. In microfluidic systems, a variety of cell properties (electrical, magnetic, dimensional, density or deformability) have been used as the physical basis for the sorting [3].

In order to identify and capture the target cell, several kinds of flow channels were designed in the microfluidic systems: electrodes, a micro-gap [4, 5], micro-holes [6], or micro-grooves [7, 8]. The photolithography technique enables manufacturing the micro-topography [9]. The movement of each cell can change at the groove on the bottom wall of the flow channel [10, 11].

In the present *in vitro* study, the movement of a single cell flowing over an oblique micro-groove, manufactured with three different groove widths, was analyzed and compared with the movement of a cell flowing outside groove.

2. METHODS

Flow Channel with Micro Grooves

For changing the movement of each flowing cell, three oblique micro grooves of the rectangular shapes (4.5 μm deep, and 0.2 mm long) have been fabricated on the surface of the polydimethylsiloxane (PDMS) plate with the photolithography technique [12]. The grooves are arranged on the bottom of the micro flow channel. The angle between the main flow direction and the longitudinal axis of the groove is 45 degrees. As to the serial groove arrangement from upstream to downstream, variation has been made on the width (w) of the groove: 0.03 mm, 0.04 mm, and 0.05 mm.

Lower Plate

The glass plate was used for the base of the mold. The epoxy based negative photo-resist material was coated on the glass. The photoresist was exposed to the UV light through the photomask in the mask aligner. After the plate was enclosed with a peripheral wall of polyimide tape, PDMS was poured with the curing agent on the plate.

[1] The authors are grateful to Prof. Richard L. Magin for assistance in the English editing of this article.

Upper Plate

The polyimide tape (0.055 mm thickness, 1 mm width, and 25 mm length) was pasted at the center of the poly-methyl-methacrylate plate for the mold. After the plate was set in the mold of poly-methyl-methacrylate, PDMS was poured with the curing agent on the plate. Two holes (diameter of 5 mm) with the interval of 20 mm were made for the inlet and the outlet.

Both the upper and the lower PDMS plates were exposed to the oxygen gas in the reactive ion etching system. Immediately after ashing, the upper disk adheres to the lower disk to make the flow path (0.05 mm high, 1 mm wide, 25 mm long) between them. The flow channel is placed on the stage of an inverted phase-contrast microscope.

Cell Flow Test

The C2C12 cell line (passage < 10, mouse myoblast cells, which originated with cross-striated muscle of C3H mice) was used in the test. Cells were pre-cultured with the D-MEM (Dulbecco's Modified Eagle's Medium) containing 10% FBS and 1% of Antibiotic-Antimycotic (penicillin, streptomycin and amphotericin B, Life Technologies) in the incubator for one week.

The inner surface of the flow channel was hydrophilized by the oxygen plasma ashing, and prefilled with a bovine serum albumin solution for thirty minutes at 310 K. Just before the flow test, the cells were exfoliated from the plate of the culture dish with trypsin and suspended in the D-MEM (Dulbecco's Modified Eagle's Medium). The suspension of cells (0.06 cm^3; 4000 cells/cm^3) was poured in the inlet of the flow channel.

The mean flow velocity (0.5 mm/s < v_c < 3 mm/s) is set by the pressure difference between the inlet and the outlet. The small reservoir (a depth of 3 mm and a diameter of 5 mm) at the inlet makes the pressure head. Each cell passing over the microgrooves was observed by the microscope, and recorded by the camera, which is set on the eyepiece of the microscope.

Analysis of Flowing Cell Movement

The coordinates are defined as follows: the direction of flow is x, the direction perpendicular to the flow is y, and the direction perpendicular to the xy-plane is z (Fig. 1). On the bottom surface of the groove, z equals zero. "ImageJ" was applied to analyze the movement of each cell. On the two-dimensional microscopic image (xy-plane), the contour of each cell was traced. The centroid was traced every 0.03 s to track the movement of the cell (Fig. 2). Using the coordinate (x, y) of the cell centroid, the velocity of the cell for the time (Δt) was calculated by Eq. (1).

$$v = (\sqrt{((x_2 - x_1)^2 + (y_2 - y_1)^2)}) / \Delta t \qquad (1)$$

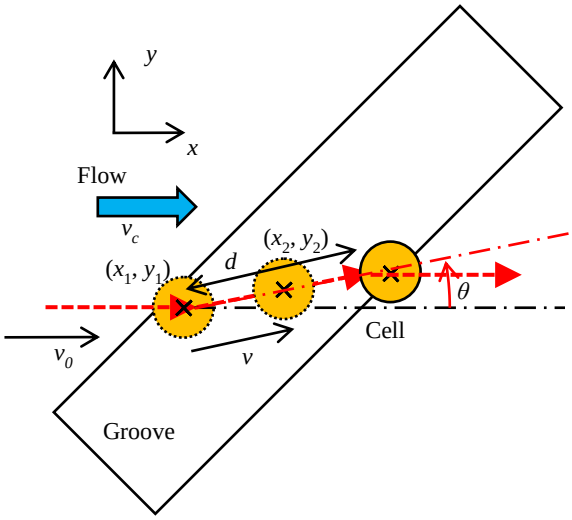

Fig. 1: Angle θ of cell movement in groove.

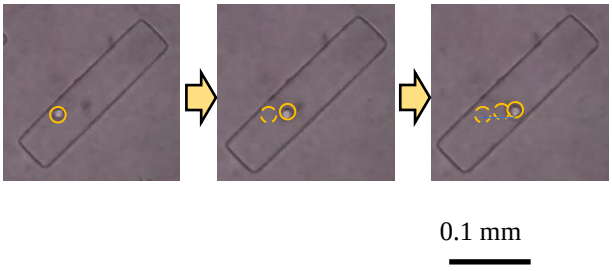

Fig. 2: Tracking of flowing cell in groove.

The cell velocity in the upstream region of grooves was measured as v_0 (Fig. 3). The velocity v_0 linearly decreases with time (t) because the pressure difference between the inlet and the outlet decreases with time. From the regression line, the mean velocity in the cross-sectional plane v_c at each timing point was calculated. The velocity ratio v_r was calculated by Eq. (2).

$$v_r = v / v_c \qquad (2)$$

The angle (−90 degrees < θ < 90 degrees) between the direction of the main flow of the medium and the velocity of each cell was measured every 0.03 s on the microscopic image.

$$\theta = \tan^{-1}((y_2 - y_1) / (x_2 - x_1)) \qquad (3)$$

When the velocity of the cell is parallel to the direction of the main flow, θ = 0 degrees. The trajectory route distance of the cell in the groove was measured as d.

The velocity distribution around grooves in the flow channel was simulated by computational fluid dynamics using "Ansys Student 2022 r2".

3. RESULTS

Fig. 3 shows relationships between the cell velocity in the upstream region of grooves (v_0) and time (t). The velocity v_0 linearly decreases with time because the pressure difference between the inlet and the outlet decreases with time. From the regression line in Fig. 3, the mean velocity in the cross-sectional plane v_c was calculated by Eq. (4).

$$v_c = -0.14\, t + 3.48 \quad (4)$$

Fig. 4 shows the results in the groove of 0.03 mm width. Fig. 4a shows the relationships between the cell velocity v and the angle θ. The angle tends to decrease with the velocity. Fig. 4b shows the relationships between the cell velocity ratio v_r and the angle θ. When the cell velocity ratio v_r is small (around the value of 0.5), the angle θ is large.

Fig. 5 shows the results in the groove of 0.04 mm width. Fig. 5a shows the relationships between the cell velocity v and the angle θ. The angle tends to decrease with the velocity. Fig. 5b shows the relationships between the cell velocity ratio v_r and the angle θ. When the cell velocity ratio v_r is small (around the value of 0.5), the angle θ is large.

Fig. 6 shows the results in the groove of 0.05 mm width. Fig. 6a shows the relationships between the cell velocity v and the angle θ. The angle decreases with the velocity. Fig. 6b shows the relationships between the cell velocity ratio v_r and the angle θ. The largest θ occurs when the cell velocity ratio v_r is small (around the value of 0.5).

Fig. 7 shows the relationships between the trajectory route distance of the cell and the angle: in the groove of 0.03 mm width (Fig. 7a), 0.04 mm width (Fig. 7b), and 0.05 mm width (Fig. 7c). The angle θ is small when the effect of the groove on cell movement is small. For example, if the cell passes away from the groove in the z-direction, the effect of the groove is small. . Even with small angles (θ), each cell travels a long distance (d) in the groove.

Figs. 8-11 illustrate the velocity distribution around grooves in the flow channel. Fig. 8 shows the velocity distribution in the xz-plane. The velocity is maximum at the center of the channel. Fig. 9 shows the velocity distribution in the yz-plane. The velocity distribution is approximately similar in the central part of the cross-section of the channel (Figs. 8 & 9). The grooves were placed in the middle 15% position, where the velocity distribution is similar.

Fig. 10 shows the velocity distribution in the xy-plane at z = 0.005 mm. The mean velocity in the cross-sectional plane in the channel is 0.5 mm/s (Fig. 10a), 1.0 mm/s (Fig. 10b), and 1.5 mm/s (Fig. 10c), respectively. The minimum velocity is illustrated in grooves in Fig 10. Fig. 11 shows the velocity distribution in the xy-plane at z = 0.01 mm. The mean velocity in the cross-sectional plane in the channel is 0.5 mm/s (Fig. 11a), 1.0 mm/s (Fig. 11b), and 1.5 mm/s (Fig. 11c), respectively. The border of the velocity distribution at the rim of the grooves becomes unclear as the mean velocity in the cross-sectional plane in the channel increases (Fig. 11c).

Calculated flow-angles α with the mean velocity v_c (0.5 mm/s < v_c < 1.5 mm/s) at different layers (z) in each groove of three different widths (30 μm, 40 μm, and 50 μm) are collected in Table 1. The value of the calculated angle α at z = 0.01 mm is close to the measured angle θ in Figs. 4-7. The height of 0.01 mm is close to the diameter of the flowing cell.

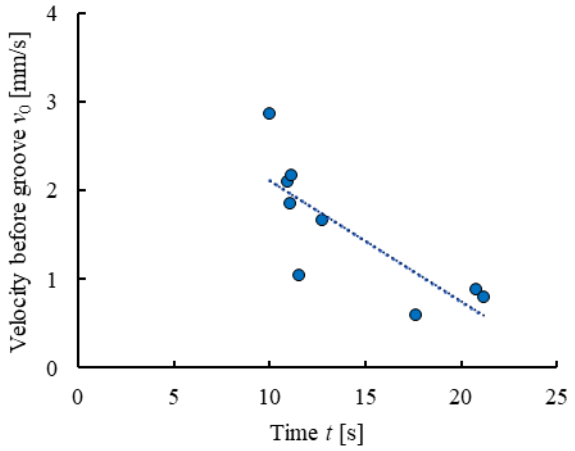

Fig. 3: Mean cell velocity before groove vs. time. Mean cell velocity decrease with time because of a decrease of the pressure head: r = 0.80: n = 9.

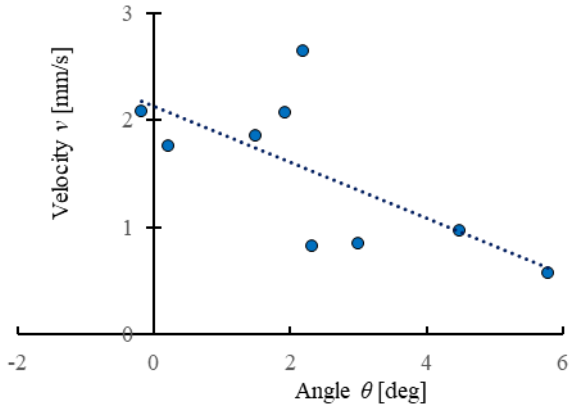

Fig. 4a: Cell velocity v vs. angle θ at groove of 0.03 mm width: $v = -0.26\,\theta + 2.13$: r = 0.68: n = 9.

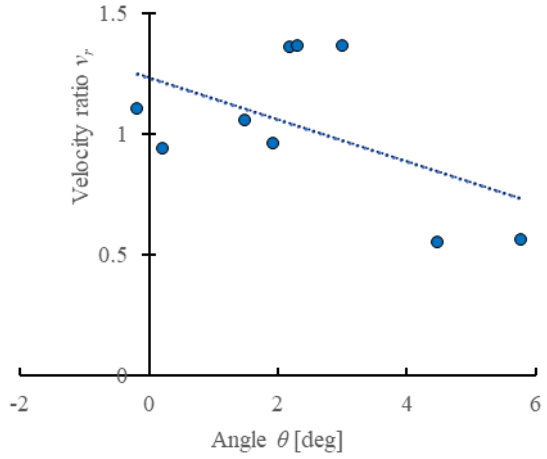

Fig. 4b: Cell velocity ratio v_r vs. angle θ at groove of 0.03 mm width: $v_r = -0.087\ \theta + 1.23$: $r = 0.51$: $n = 9$.

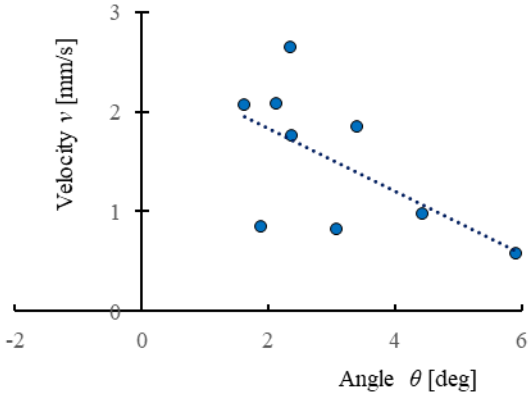

Fig. 5a: Cell velocity v vs. angle θ at groove of 0.04 mm width: $v = -0.31\ \theta + 2.46$: $r = 0.60$: $n = 9$.

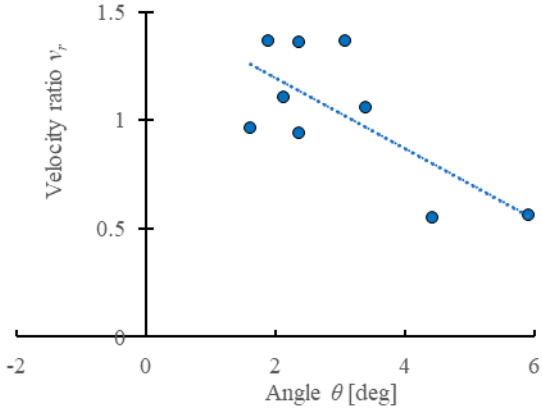

Fig. 5b: Cell velocity ratio v_r vs. angle θ at groove of 0.04 mm width: $v_r = -0.16\ \theta + 1.52$: $r = 0.71$: $n = 9$.

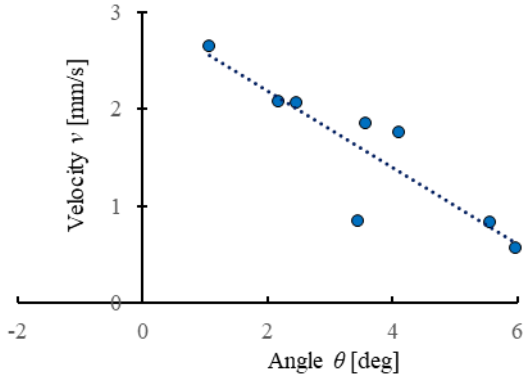

Fig. 6a: Cell velocity v vs. angle θ at groove of 0.05 mm width: $v = -0.39\ \theta + 2.98$: $r = 0.88$: $n = 8$.

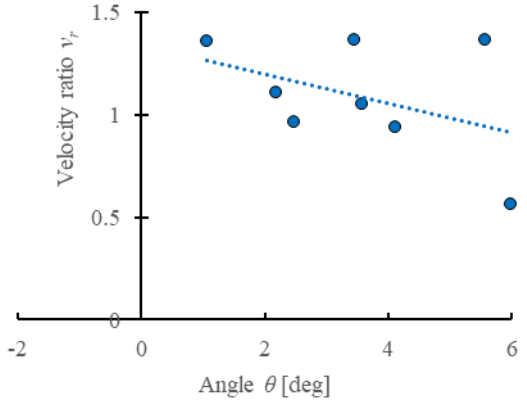

Fig. 6b: Cell velocity ratio v_r vs. angle θ at groove of 0.05 mm width: $v_r = -0.072\ \theta + 1.34$: $r = 0.43$: $n = 8$.

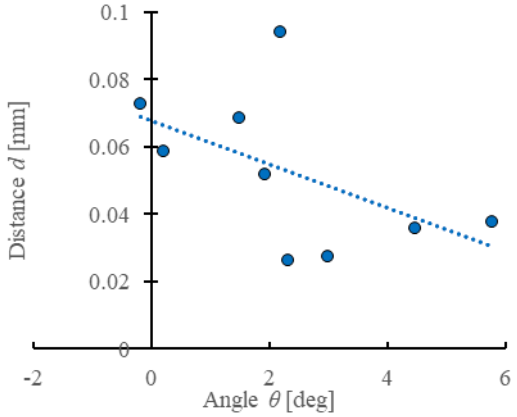

Fig. 7a: Trajectory route distance in groove d vs. angle θ at groove of 0.03 mm width: $d = -0.0065\ \theta + 0.068$: $r = 0.53$: $n = 9$.

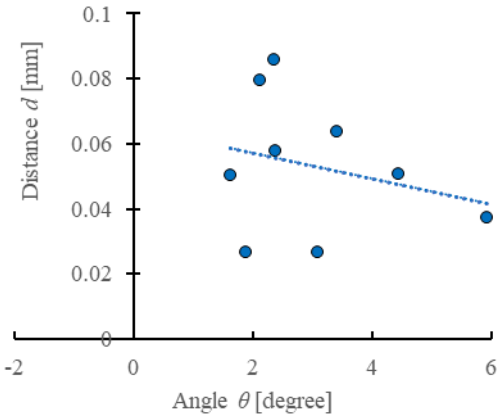

Fig. 7b: Trajectory route distance in groove d vs. angle θ at groove of 0.04 mm width: $d = -0.004\ \theta + 0.065$: $r = 0.26$: $n = 9$.

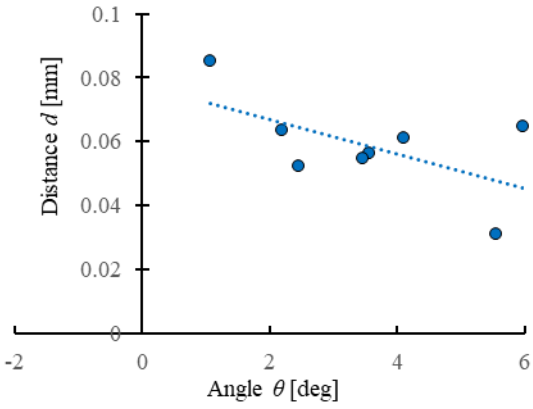

Fig. 7c: Trajectory route distance in groove d vs. angle θ at groove of 0.05 mm width: $d = -0.0054\ \theta + 0.078$: $r = 0.60$: $n = 8$.

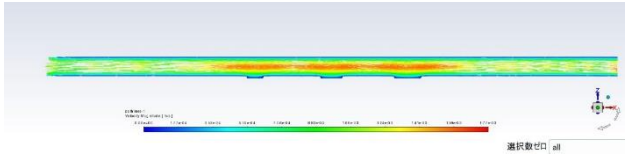

Fig. 8: Velocity distribution in *xz*-plane.

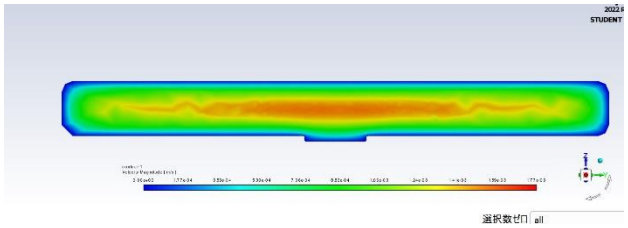

Fig. 9: Velocity distribution in *yz*-plane.

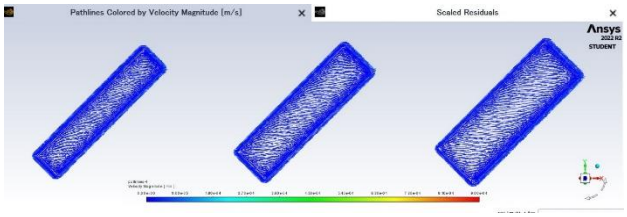

Fig. 10a: Velocity distribution in *xy*-plane at $z = 0.005$ mm, $v_c = 0.5$ mm/s: $\alpha = 12.3$ deg, 7.4 deg, 5.0 deg.

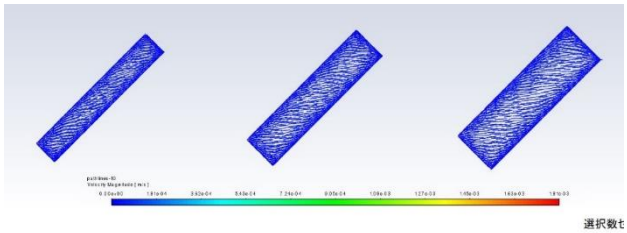

Fig. 10b: Velocity distribution in *xy*-plane at $z = 0.005$ mm, $v_c = 1.0$ mm/s: $\alpha = 12.6$ deg, 7.5 deg, 5.5 deg.

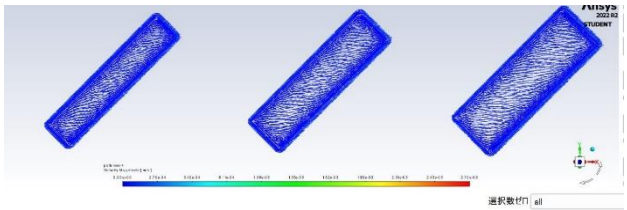

Fig. 10c: Velocity distribution in *xy*-plane at $z = 0.005$ mm, $v_c = 1.5$ mm/s: $\alpha = 12.1$ deg, 7.8 deg, 5.5 deg.

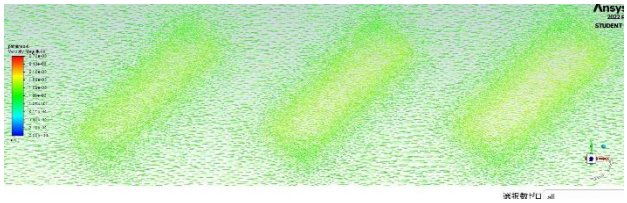

Fig. 11a: Velocity distribution in *xy*-plane at $z = 0.01$ mm, $v_c = 0.5$ mm/s: $\alpha = 4.6$ deg, 3.0 deg, 1.8 deg.

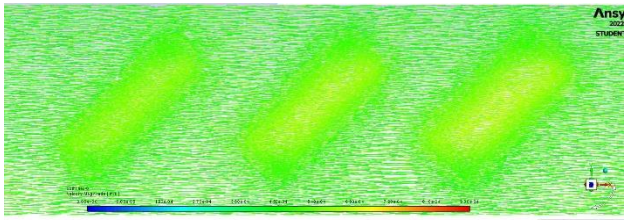

Fig. 11b: Velocity distribution in *xy*-plane at $z = 0.01$ mm, $v_c = 1.0$ mm/s: $\alpha = 4.2$ deg, 3.4 deg, 2.8 deg.

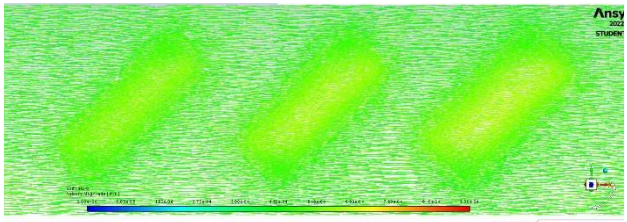

Fig. 11c: Velocity distribution in *xy*-plane at $z = 0.01$ mm, $v_c = 1.5$ mm/s: $\alpha = 6.3$ deg, 4.3 deg, 3.6 deg.

Table 1: Calculated flow direction angle α at different layers (z) in each groove (width) of three different widths: 0.5 mm/s < v_c < 1.5 mm/s.

z mm	α(30 μm) deg	α(40 μm) deg	α(50 μm) deg
0.005	12	7	5
0.01	5	4	3

4. DISCUSSION

Filtration and cell staining are basic methods used in cell sorting. The fluorescence techniques commonly used in flow cytometry, for example, require cell fixation. Non-destructive cell sorting systems, on the other hand, were designed in the previous studies [4-7]. The label-free methods were designed with microfluidic systems [13]. Some of them were designed to capture cancer cells [2].

Several different fluid flow and cell capture systems have been used in the previous studies [14]. In one of our previous studies [6], cylindrical and half-cylindrical holes were used to trap cells. In that study, an asymmetrical hole might be a better way to to trap cells than a symmetrical hole.

In the previous study [9], rectangular grooves have been successfully manufactured on the wall of the micro fluid channel. The dimensions of the grooves were confirmed by the laser microscope. The depths of the micro patterns were between 2 μm and 10 μm in the previous studies. In the present study, the depth of the grooves is 4.5 μm, which is smaller than the diameter of the cells. The deeper hole may provide a better way to trap cells. For a shallower trap, on the other hand, it is not easy to trap a cell.

The depth of the groove may be an appropriate dimension to distinguish cells. The duration of the trapped time of the cell might also depend on the interaction between the micro hole and the cell; as well as the affinity between the cell and the surface of the micro pattern, or deformability of the cell.

The results of another previous study [10] showed that the movement of cells travelling on the wall is modified by the oblique micro groove on the wall under the cell for velocities lower than 1 mm/s. A groove angle of 45 degrees between the longitudinal direction of the groove and the flow direction was found to shift the streamline of the cell. This behavior is supported the flow around the groove displayed in Fig. 11.

The bumping movement of the cell over the oblique groove depends on several parameters: the diameter of cells, the width of the groove, the velocity of the cell, and the shape of the cell [8]. The movement of cells on the bottom surface of the flow channel may be related to the specific gravity (the density difference between the cell and the medium) of the cell.

In another of our previous studies [10], the shifted distance of malnourished cells by the oblique groove was smaller than that of normal cells. Hence, the shape of a flowing cell can be detected by its movement over a micro groove. In addition, the stepwise movement of cells increased with an increase in the groove angle; a tendency was more evident in a wider groove.

In this study, the velocity distribution is relatively uniform in the central part of the cross-section of the channel (Figs 8 & 9), except for wall effects and at the entrance region. Therefore, the grooves were placed in the middle 15% position, where the velocity distribution is more uniform.

Finally, we found that a small v_r corresponded to the flow velocity near the bottom of the channels (Figs. 4b, 5b, 6b). Cells along the top side were not included as they were out of focus in the image and a cell velocity ratio v_r larger than one corresponds to the core flow velocity. Scatter of data for the velocity ratio v_r larger than one might depend on the distance in z direction from the microgroove.

The height (z direction) of the flow channel should be closer to the diameter of the flowing cell so that the effects of the flow velocity distribution in z direction are minimized. These findings, and the data shown in Fig. 7, illustrate the influence of groove width on cell trajectory, distance d, which could be used to sort cells.

5. CONCLUSIONS

A micro flow-channel with oblique microgrooves of different witdths was manufactured using the PDMS micromachining. The bumping movement of the cell flowing over the oblique micro groove was recorded and analysed. The experimental results showed a direction change for each cell as it passed along the micro groove; a change whose magnitude depended on the flow velocity and on the width of the groove. This behavior demonstrates how micro flow-channels fabricated with oblique grooves have the potential to be applied for sorting cells.

ACKNOWLEDGMENT

The authors thank Mr. Akira Hayasaka for the help of the experiment.

REFERENCES

[1] C.W. Shields, K.A. Ohiri, L.M. Szott and G.P. López, "Translating Microfluidics: Cell Separation Technologies and Their Barriers to Commercialization", **Cytometry Part B, Clinical Cytometry**, Vol. 92, No. 2, 2016, pp. 115-125.

[2] H. Andersson and A. van den Berg, "Microfluidic Devices for Cellomics: A Review", **Sensors and Actuators B: Chemical**, Vol. 92, No. 3, 2003, pp. 315-325.

[3] S. Byun, V.C. Hecht and S.R. Manalis, "Characterizing Cellular Biophysical Responses to Stress by Relating Density, Deformability, and Size", **Biophysical Journal**, Vol. 109, No. 8, 2015, pp. 1565-1573.

[4] S. Hashimoto, "Cell Behavior in Flow Passing through Micromachined Gap", **ASME Journal of Engineering and Science in Medical Diagnostics and Therapy**, Vol. 5, No. 4(041001), 2022, pp. 1-6. (DOI 10.1115/1.4054261)

[5] S. Uehara, S. Hashimoto, S. Shimada and A. Kurihara, "Cell Behavior During Accelerated Passing through Micro-gap", **Journal of Systemics Cybernetics and Informatics**, Vol. 20, No. 3, 2022, pp. 24-30. (DOI 10.54808/JSCI.20.03.24)

[6] S. Hashimoto, Y. Takahashi, H. Hino, R. Nomoto and T. Yasuda, "Micro Hole for Trapping Flowing Cell", **Proc. 18th World Multi-Conference on Systemics Cybernetics and Informatics**, Vol. 2, 2014, pp. 114-119.

[7] S. Hashimoto, "Behavior of Cell Flowing Over Oblique Microrectangular Groove", **ASME Journal of Engineering and Science in Medical Diagnostics and Therapy**, Vol. 5, No. 4(041008), 2022, pp. 1-8. (DOI 10.1115/1.4055016)

[8] S. Hashimoto, T. Matsumoto and S. Uehara, "How Does a Cell Change Flow Direction Due to a Micro Groove?", **Journal of Systemics Cybernetics and Informatics**, Vol. 19, No. 8, 2021, pp. 164-181. (DOI 10.54808/JSCI.19.08.164)

[9] P.N. Carlsen, **Polydimethylsiloxane: Structure and Applications**, Nova Science Publishers, 2020, pp. 29-94.

[10] S. Hashimoto, A. Hayasaka and Y. Endo, "Sorting of Cells with Flow Channel: Movement of Flowing Myoblast Cell at Oblique Micro Grooves", **Proc. 23rd World Multi-Conference on Systemics Cybernetics and Informatics**, Vol. 4, 2019, pp. 82-87.

[11] S. Hashimoto, S. Kuwabara, H. Yonezawa and Y. Endo, "Effect of Shape of Cell on Movement over Micro Groove in Flow Channel", **Proc. 12th International Multi-Conference on Complexity Informatics and Cybernetics**, Vol. 2, 2021, pp. 19-24.

[12] S. Hashimoto, T. Matsumoto, S. Uehara and Y. Endo, "Bumping Movement of Cell Flowing over Oblique Micro-groove: Comparison with Movement Outside Groove", **Proc. 13th International Multi-Conference on Complexity Informatics and Cybernetics**, Vol. 2, 2022, pp. 23-28.

[13] L.R. Huang, E.C. Cox, R.H. Austin, and J.C. Sturm, "Continuous Particle Separation through Deterministic Lateral Displacement," **Science**, Vol. 304, No. 5673, 2004, pp. 987-990.

[14] H. Ramachandran, S. Martins, Z. Kontarakis, J. Krutmann and A. Rossi, "Fast But Not Furious: A Streamlined Selection Method for Genome-edited Cells", **Life Science Alliance**, Vol. 4, No. 6, 2021, pp. 1-7.